ABSOLUTE ROVIBRATIONAL INTENSITIES, SELF-BROADENING AND SELF-SHIFT COEFFICIENTS FOR THE $X^1\Sigma^+$ V=3← V=0 BAND OF $^{12}C^{16}O$

C. Chackerian, Jr., NASA Ames Research Center and
SETI Institute
Atmospheric Physics Branch
MS 245-4, Moffett Field, CA 94035-1000

R. Freedman, NASA Ames Research Center and
Space Physics Research Institute
MS 245-3, Moffett Field, CA 94035-1000

L. P. Giver, NASA Ames Research Center
Atmospheric Physics Branch
MS 245-4, Moffett Field, CA 94035-1000

and

L. R. Brown
Jet Propulsion Laboratory
California Institute of Technology
4800 Oak Grove Drive, Pasadena, CA 91109

Running head: CO 3-0 band: intensities, self shifts and self broadening.

Proofs should be sent to: Charles Chackerian, Jr.
NASA Ames Research Ctr, MS 245-4, Moffett Field, CA 94022
650-604-6300; 650-604-3625 (FAX)
cchackerian@mail.arc.nasa.gov

Abstract: The rotationless transition moment squared for the $X^1\Sigma^+$ v=3←v=0 band of CO is measured to be $|R_{3-0}|^2$ = 1.7127(25)x10^{-7} Debye^2. This value is about 8.6 percent smaller than the value assumed for HITRAN 2000. The Herman-Wallis intensity factor of this band is F=1+0.01168(11)m+0.0001065(79)m^2. The determination of self-broadening coefficients is improved with the inclusion of line narrowing; self-shifts are also reported.

1. INTRODUCTION

Rovibrational intensities for the ground electronic state of carbon monoxide that appear in the current version of HITRAN and HITEMP cover a large range of vibrational quantum numbers, 0≤v≤22 with Δv=1-4, and rotational quantum numbers, 0 ≤ J ≤ 150. These intensities reported by Goorvitch (1) and Goorvitch and Chackerian (2,3) are based on the electric dipole moment function (EDMF) reported by Chackerian *et al.* (4) in 1983. The EDMF (4) was obtained via a number of experimental measurements of absolute and relative intensities. Included in the measurements was the v=3←v=0 band transition moment squared, $|R_{3-0}|^2$, for $^{12}C^{16}O$ determined by Toth *et al.* (5) in 1969. Subsequently Bouanich *et al.* (6) in 1983 redetermined $|R_{3-0}|^2$ via spectra which they recorded with CO densities between 47 and 140 amagat. The resultant $|R_{3-0}|^2$ obtained by Bouanich *et al.* (6) is about 6 percent smaller than that determined by Toth *et al.* (5).

Intensity work done on the v=3←v=0 band of carbon monoxide previous to 1983 is summarized by Bouanich *et al.* (6,7)

More recently two groups, Picqué and Guelachvili (8) using a FTS and Henningsen *et al.* (9) using a diode laser, both obtained a value of $|R_{3-0}|^2$ about 8-10 percent smaller than the value reported by Toth et *al.* (5). Since we have recently obtained results of $|R_{2-0}|^2$ for CO (10) which also differ from the value we used to determine the EDMF of CO (4), we decided to check the recent intensity results for the v=3←v=0 band before redetermining the EDMF. This redetermined EDMF will then be used to improve the accuracy of the CO rovibrational line intensities listed in HITRAN.

In addition to the line intensities for the v=3←v=0 band, we have also determined the self-shift and self-broadening coefficients. The fits of line profiles showed evidence of line narrowing, but the signal to noise of the spectra was not sufficient to determine these parameters. Improved fits were obtained, however, assuming the narrowing parameters we have determined via spectra of the v=2←v=0 band which were recorded with high signal to noise ratios. Henningsen *et al.* (9) also determined R-branch self-broadening widths and shifts and Picqué and Guelachvili (8) reported self-broadening widths and shifts

for the v=3←v=0 band as well. The latter previously (11) reported line frequency and self-shift coefficients. Quite recently Jacquemart *et al.* (12) have obtained direct measurements of narrowing parameters for the v=3←v=0 band using the same spectra of Ref. (8).

2. EXPERIMENTAL

Spectra were recorded with the FTS instrument at the Kitt Peak, AZ National Solar Observatory. The conditions of optical path length, gas pressure, temperature and spectral resolution used to obtain these spectra are given in Table 1. Both a straight 1.5 m tube and a White-type multiple reflection cell, with a nominal 6 m base path, were used for absorption cells.

The three high-pressure spectra were recorded using InSb detectors, a CaF2 beam splitter and integration times of 1.6 hours. The two low-pressure scans were taken in order to validate measurements involving the O_2 A-band at 13100 cm^{-1} (13). For the latter set, spectra were recorded with a fused silica beam splitter, and the simultaneous use of one InSb and one Si diode detector with integration times of 1.1 hours.
Temperatures were monitored using thermistors in thermal contact with the exterior of the absorption cells, and these readings are accurate to 1 K. Pressures were measured with 10

and 1000 torr MKS baratron gauges calibrated to 0.5% or better. Gas purity was 99.5%.

3. ANALYSIS

Individual rovibrational intensities, S_{obs}, were determined by non-linear least-squares fits of the transmission of recorded lines assuming a Beer-Lambert law,

$$\frac{I(\Delta\sigma = \sigma - \sigma_o)}{I_o(\sigma)} = \exp\left[-S_{obs} pl \frac{H(\Delta\sigma, Y)}{\gamma_D} \left(\frac{\ln 2}{\pi} \right)^{1/2} \right]. \quad [1]$$

The transmission profile represented by Eq. [1] was convolved by a box-car instrumental function which accounts for the finite FTS aperture as well as a phase error, according to the formulation of Dana and Mandin (14). Optimized values for the finite aperture and phase parameters were determined from the two low pressure spectra (KP13, KP14) and held fixed for fits of the individual lines on spectra recorded at higher pressures (KP21, KP23, KP24). A typical fit, shown in Fig. (1) will be discussed in more detail below.

In Eq. [1] $I_o(X)$ and $I(X)$ are the intensities respectively, incident on and emergent from the absorbing gas sample. S_{obs} is the line intensity, p the total

CO gas pressure (atm.), l the absorbing path length (cm), and H(X,Y,Z) the Voigt-Galatry line shape. The Voigt-Galatry line shape parameters for frequency, $\nu(cm^{-1})$, line center frequency, $\nu_o(cm^{-1})$, broadening coefficient, $\gamma(cm^{-1}/atm)$, and narrowing coefficient, $\beta(cm^{-1}/atm)$, are, $X = \left(\left[\nu - \nu_o\right]/\gamma_D\right)\sqrt{\ln 2}$, $Y = (\gamma_L/\gamma_D)\sqrt{\ln 2}$, and $Z = \beta/\gamma_D$ respectively. The Doppler broadening coefficient, $\gamma_D(cm^{-1})$, and pressure broadening coefficient, γ_L, are both defined as the respective profile half-width at half maximum depth. A computer code supplied by Herbert (15) was used to compute the H(X,Y,Z) function.

Except for β, the parameters, ν_o, γ_L, and S_{obs}, were determined via non-linear least-squares fits of the convolved spectra. Pressure shifts, δ, of the spectral lines were also determined. We will discuss the different parameters in sections below.

3a. Intensities.

Line intensity values, S_{obs}, were obtained for each of the spectra in Table 1 for m values in the range $-18 \le m \le 23$. Here m is -J or J+1 for P- and R-branch transitions, respectively. The individual line intensities were all converted to the common temperature of T= 296 K via Eq. [2],

$$\frac{S(m,296)}{S(m,T)} = \frac{TQ_{vr}(T)}{296Q_{vr}(296)} \exp\left[-1.4388E''\left(1/296 - 1/T\right)\right] \quad [2]$$

, where E" is the transition lower state energy (cm^{-1}), and $Q_{vr}(T)$ the rovibrational partition function at temperature T(Kelvin). $Q_{vr}(T)$ values were taken from Ref. (16) and Q(296)=107.427. The intensities determined for the five spectra were then averaged for each m value with a standard deviation calculated according to Eq. [3],

$$sd(S_{obs}) = \frac{1}{2}\left[\Sigma_i\left(S_{avg} - S_i\right)^2\right]^{1/2}. \quad [3]$$

The averaged observed values of the line intensities are presented for the isotope $^{12}C^{16}O$ in Table 2.

The rotationless transition moment squared, $|R_{3-0}|^2$(Debye^2), and Herman-Wallis intensity parameters, C and D, were obtained from quadratic fits of the reduced intensity, S_{red}, given by Eqs. [4], plotted against the quantum number m.

$$S_{red}(m) = \frac{S_{obs}\left(3.27368x10^{-4}\right)Q_{vr}(T)T}{\sigma L(m)} e^{hcE''/kT} \quad [4].$$

$$S_{red}(m) = \left|R_{3-0}\right|^2 \bullet \left(1 + Cm + Dm^2\right)$$

In Eq. [4] E" is the lower state energy (cm^{-1}), v the frequency (cm^{-1}) and L(m) is |-J| or |J+1| for P- and R-branch transitions, respectively. Transition frequencies and lower state energies (cm^{-1}) were taken from HITRAN 1996 and are based on Farrenq *et al.* (17). A plot of the reduced intensity versus m is shown in Fig. 2.

A comparison of intensity factors, $|R_{3-0}|^2$, C, and D, with previous results are given in Table 3. The $|R_{3-0}|^2$ value from Ref. (9) has been adjusted to account for the fact that these authors used a slightly different partition function and reported values for natural abundance rather than pure sample. The more modern measurements of $|R_{3-0}|^2$ fall about 8.6 percent below the value of Toth *et al.* (5) which is the basis of the current HITRAN CO line intensities. References (8) and (12) represent the same data set treated in slightly different ways: the former with Voigt profiles and spectra analyzed one at a time and the latter with a multi-spectral fit and Galatry profiles. The measured Herman-Wallis factors, C and D, determined by Picqué *et al.* (8) seem to be in best agreement with those calculated from a new electric dipole moment function (18) (EDMF) we have obtained from inclusion of experimental data obtained since our last publication of the CO EDMF (4). The intensity parameters we have determined and which are listed in Table 3 reproduce our measurements on average to a RMS better than 0.4 percent as can be seen from the last column of Table 2.

3b. Pressure shifts.

The pressure shifts were obtained in two steps. In the first step the frequency scale of each spectrum was independently calibrated. Water lines were used as frequency standards for the three spectra obtained with the 1.5 m cell. These lines were present because of residual water in the vacuum tank of the FTS; their frequencies had previously been determined (19,20) to an accuracy of about 0.0001 cm^{-1}. The $v=3 \leftarrow v=0$ (11) and $v=2 \leftarrow v=0$ (20) bands of CO were used for frequency standards for spectra obtained with the multiple reflection cell. The corrections applied to the frequencies ranged from multiplying the observed "raw" values by factors in the range 1.000000126 to 1.000000206.

The slopes of plots of the corrected frequencies versus total gas pressure were taken as the frequency shift, $\delta(cm^{-1}/atm)$; an example of such a plot is given in Fig. (3) for the m=-14 transition. The intercepts of the plots give the vacuum frequencies and for all but a few lines the vacuum intercepts obtained from the plots represented by Fig. (3) are in excellent agreement with the calculated and observed results reported by Picqué, and

Guelachvili (11). The intercept of this plot in Fig. 3, 6393.176740(14) cm^{-1}, is acceptably close to the result, 6393.176687 cm^{-1}, reported by Picqué *et al.* (8,11). The largest difference in vacuum frequencies between the latter (11) and our measurements is 0.0002 cm^{-1} but the differences are mostly 0.0001 cm^{-1} and smaller.

The shifts we determined are tabulated in the fourth and eighth columns of Table 4 and are shown plotted versus m in Fig. (4) as well. Also shown on Fig. (4) are results obtained by Picqué and Guelachvili (11) and by Henningsen *et al.* (9). The former estimate an uncertainty in their individual shift measurements on the order of $\pm 50 \times 10^{-5}$ cm^{-1}/atm and the latter about $\pm 65 \times 10^{-5}$ cm^{-1}/atm. The standard deviation between the 36 points in common between (11) and this work is 41×10^{-5} cm^{-1}/atm. The results shown for Henningsen *et al.* (9) have been smoothed via a fit by those authors. Considering the quoted errors, the results shown on Fig. (4) are in good agreement.

Figure 5 is a presentation of our shift data plotted versus |m|. This figure indicates that the P-branch shifts are on the order of eight percent larger than the R-branch shifts. Such a trend seems to be independent of collision partner as well as upper-state vibrational quantum number, v, in the series of fundamental and overtone vibrational bands of CO, $v \leftarrow 0$ (21-24). The average shift we

obtained for the 3←0 band with $-18 \leq m \leq 21$ is -598×10^{-5} cm^{-1}/atm. It is interesting to note that the average shift obtained by Predoi-Cross *et al.* (24) for the same m range, but for the 2←0 band, is -421×10^{-5} cm^{-1}/atm. The ratio of the average shifts, $\langle\delta(3\leftarrow0)\rangle/\langle\delta(2\leftarrow0)\rangle$, is equal to 1.44 while the ratio of the purely vibrational energies is about 1.50. The measurements of Predoi-Cross were somewhat corroborated by Bouanich et al. (22) who measured 18 lines between m = -7 and m = 22 with an average shift of -391×10^{-5} cm^{-1}/atm. A similar ratio, using the data of Devi *et al.* (23) for the 1←0 band, gives 3.3 while the ratio of vibrational energies is about 2.98. New measurements (26) on the 1←0 band indicate that these shifts should be somewhat larger than indicated in reference (23).

3c. Self pressure-broadening coefficients.

The dotted line connecting unfilled circles in Fig. 1. is the fitted profile minus the observed spectral profile. For this fit a Voigt line shape, $H(X,Y,0)$, was used. The characteristic "w" in this difference curve indicates the presence of narrowing which amounts to about 0.5 percent on the transmission scale (see right-hand abscissa). As can be seen from this figure, the oscillatory-like deviations of the observed and fitted spectra in the line wings are large enough to prevent a determination of the narrowing parameter, β. However, we found that we

could improve the fits slightly by adopting the β coefficients we have determined from much higher signal to noise spectra of the 2←0 band. For completeness these coefficients are listed in Table 4. The determination of these β values will be discussed in a future publication (10). The filled diamonds in Fig. 1 show the differences between the fitted and observed line profile using the appropriate fixed value of β taken from Table 4.

The individual broadening coefficients, γ_L, given in Table 4 were obtained from the slopes of plots of the broadening, observed at each pressure, versus pressure. We used the KP21, KP23, and KP24 spectra and found that the zero-pressure intercepts on the plots with three points scattered about zero by small amounts. Therefore, we added a fourth point, zero broadening at zero pressure, to obtain our final results for the pressure broadening coefficients. Figure 6 compares these measurements with those of others. Henningsen *et al.* (9) used a New Focus external-cavity diode laser and corrected for the effects of collisional narrowing(~0.6 percent effect). Jacquemart *et al.* (12) reanalyzed the FTS spectra of Picqué *et al.* (8) by simultaneously fitting all of their spectra as well as including line narrowing. With a few exceptions the three determinations seem to be in excellent agreement.

Figure 7 compares self-broadening coefficients of the fundamental and first two overtones of CO. The results obtained for the v=2←v=0 band by Predoi-Cross *et al.* (23)

are nearly indistinguishable from those we have measured for the v=3←v=0 band. Previous work on the v=2←v=0 band has been reviewed by Predoi-Cross *et al.* (23) and is in good agreement with their results. The results obtained by Nakazawa and Tanaka (26) for the v=1←v=0 band similarly is in good agreement with measurements on the overtones. On the other hand results for the v=1←v=0 band obtained by Devi *et al.* (23) are systematically larger by ~ 0.0045 cm^{-1}/atm.

4. CONCLUSION

The average $|R_{3-0}|^2$ value for the modern measurements, this work and references (11) and (12), equals $(1.694\pm0.016)\times10^{-7}$ D^2. The standard deviation on this average indicates that the transition moment squared of the v=3←v=0 band is probably known to on the order of 1-2 percent. Further improvements in absolute intensity measurements will result from very close attention being paid to the accuracy of the sample pressure, temperature and composition.

The rotationless transition moment we have determined for the v=3←v=0 band of $^{12}C^{16}O$ is 7.4 percent smaller than Toth *et al.* (5) which was assumed in the determination of the EDMF of the $X^1\Sigma^+$ state of carbon monoxide (4). The latter in turn forms part of the basis for all of the CO intensities in the current versions of HITRAN

and HITEMP. A new determination of the EDMF will be carried out using these and other currently new intensity data on CO (18).

Self-pressure shifts for the $v=3\leftarrow v=0$ and $v=2\leftarrow v=0$ bands are close to being in proportion to their vibrational energies (band centers). This proportion does not seem to hold as well with the $v=1\leftarrow v=0$ band but newer data may bring the $v=1\leftarrow v=0$ band into better agreement with this empirical "rule".

Self-pressure broadening coefficients for the $v=3\leftarrow v=0$ band are in good agreement with two recent determinations and the self-broadening in CO appears to be independent of n in the $v=n\leftarrow v=0$, n=1,2,3, series of transitions.

ACKNOWLEDGEMENT

Part of the research described in this paper was performed at the Jet Propulsion Laboratory, California Institute of Technology under contract with The National Aeronautics and Space Administration.

5. REFERENCES

1. D. Goorvitch, Ap. J. Supplement **95**, 535-552 (1994).

2. D. Goorvitch and C. Chackerian, Jr., Ap. J. Suppl. Series **91**, 483-489 (1994).

3. D. Goorvitch and C. Chackerian, Jr., Ap. J. Supplement **92**, 311-321 (1994).

4. C. Chackerian, Jr., R. Farrenq, G. Guelachvili, C. Rossetti, and W. Urban, Can. J. Phys. **62**, 1579-1585 (1984).

5. R. A. Toth, R. H. Hunt and E. K. Plyler, J. Mol. Spectrosc. **32**, 85-96 (1969).

6. J.-P. Bouanich, N-V Thanh, and I. Rossi, JQSRT **30**, 9-15 (1983).

7. J.-P. Bouanich and C. Brodbeck, JQSRT **14**, 1199-11208 (1974).

8. N. Picqué, and G. Guelachvili, V. Dana, and J.-Y. Mandin, J. Mol. Structure **517-518** 427-434 (2000).

9. J. Henningsen, H. Simonsen, T. Møgelberg and E. Trudsø, J. Mol. Spectrosc. **193**, 354-362 (1999).

10. C. Chackerian, Jr. R. Freedman, L. R. Brown. and J. W. Brault (to be published).

11. N. Picqué and G. Guelachvili, J. Mol. Spectrosc. **185**, 244-248 (1997).

12. D. Jacquemart, J.-Y. Mandin, N. Picqué, and G. Guelachvili, Eur. Phys. J. D **14**, 55-69 (2001).

13. L. R. Brown and C. Plymate,
J. Mol. Spectrosc. **199**, 166-179 (2000).

14. V. Dana and J.-Y. Mandin, JQSRT **48**, 725-731 (1992).

15. F. Herbert, JQSRT **14**, 943-9xx (1974).

16. C. Chackerian, Jr., G. Guelachvili, and R. H. Tipping,
JQSRT **30**, 107-112 (1983).

17. R. Farrenq, G. Guelachvili, A. J. Sauval, N. Grevesse, and
C. B. Farmer, J. Mol. Spectrosc. **149**, 375-390 (1991).

18. C. Chackerian, Jr. and R. Freedman (to be published).

19. L. R. Brown and J. S. Margolis, JQSRT **56**, 4791-5294
(1996).

20. C. R. Pollock, F. R. Petersen, D. A. Jennings, J. S. Wells,
and A. G. Maki, J. Mol. Spectrosc. **99**, 357-368 (1983).

21. J.-P. Bouanich and C. Brodbeck, JQSRT **13**, 1-7 (1972).

22. J.-P. Bouanich, D. Bermejo, J. L. Domenech, R. Z.
Martinez, and J. Santos, J. Mol. Spectrosc. **179**, 22-31
(1996).

23. V. M. Devi, D. C. Benner, M. A. H. Smith, and C. P.
Rinsland, JQSRT **60**, 815-824 (1998).

24. A. Predoi-Cross, J.-P. Bouanich, D. C. Benner, A. D. May,
and J. R. Drummond, J. Chem. Phys. **113**, 158-168
(2000).

25. M. A. H. Smith, (Private communication).

26. T. Nakazawa and M. Tanaka, JQSRT **28**, 409-416 (1982).

6. FIGURE CAPTIONS

Fig. 1. Non-linear least-squares fit of the $^{12}C^{16}O$ V=3←V=0, m = +9 line transmission. Right-hand abscissa shows differences$x10^3$ between fitted and observed transmission. Spectrum KP24. Open circles: (fitted - observed) with a Voigt line shape. Filled diamonds: (fitted -observed) with a Galatry line shape.

Fig. 2. Reduced intensity vs. m for the v=3←v=0 band of $^{12}C^{16}O$

Fig. 3. Observed frequency of the m = -14 line versus pressure.

Fig. 4. Self-shift coefficients versus m for the CO v=3←v=0 band. Filled diamonds: this work; error bars represent one standard deviation. Unfilled diamonds connected with dashed lines: Picqué and Guelachvili (11). Dashed curve: Henningsen et al.'s (9) fit of their data.

Fig. 5. Self-shift coefficients versus |m| for the CO v=3←v=0 band. Filled diamonds: R branch; unfilled diamonds: P branch. Error bars represent one standard deviation.

Fig. 6. Self-broadening coefficients versus m for the CO v=3←v=0 band. This work, open circles. Error bars represent one standard deviation. Solid curve, connects R-branch values obtained by Henningsen et al. (9). Solid diamonds, Picqué and Guelachvili (12).

Fig. 7. Self-broadening coefficients versus |m| for the CO v=3←v=0, v=2←v=0, and v=1←v=0 bands. (3←0) this work: circles, P branch; filled diamonds, R branch. (2←0) Predoi-Cross *et al.* (24):dashed line, P branch; solid line, R branch. (1←0) Devi *et al.* (23): open diamonds connected by dashed lines, P branch; open diamonds connected by solid lines, R branch. (1←0) T. Nakazawa and M. Tanaka (26): double unfilled triangles, R branch.

TABLES

Table 1. Experimental Conditions.

Spectrum[a]	Path (M)	P(Torr)	T(K)	Res. (cm^{-1})
KP13	73	3.11	294.3(1.6)	0.020
KP14	73	6.71	295.0(1.8)	0.020
KP21	1.5	401.4	296.3(0.5)	0.0109
KP23	1.5	298.2	297.6(0.5)	0.0109
KP24	1.5	204.6	296.9(0.5)	0.0109

[a]Interferograms are double-sided.

Table 2. Observed[a] and Calculated[b] Line Intensities[c] at 296 K.

m	$\sigma(cm^{-1})$	S(obs)x10^4	S(calc) x10^4	Comparison[d]
-18	6265.3043	0.649(30)	0.628	3.3[e]
-17	6270.9120	0.843(37)	0.839	0.5
-16	6276.4173	1.103(29)	1.110	-0.6
-15	6281.8198	1.403(47)	1.399	0.3
-14	6287.1196	1.753(44)	1.747	0.3
-13	6292.3163	2.130(43)	2.130	0.0
-12	6297.4100	2.512(54)	2.535	-0.9
-11	6302.4005	2.933(51)	2.940	-0.2
-10	6307.2875	3.327(41)	3.320	-0.2
-9	6312.0710	3.639(70)	3.643	-0.1
-8	6316.7509	3.880(45)	3.876	0.1
-7	6321.3268	3.978(25)	3.984	-0.2
-6	6325.7989	3.914(25)	3.938	-0.6
-5	6330.1667	3.693(48)	3.715	-0.6
-4	6334.4303	3.309(22)	3.303	0.2
-3	6338.5895	2.707(29)	2.702	0.2
-2	6342.6441	1.936(20)	1.928	0.4
-1	6346.5940	1.012(10)	1.013	-0.1
1	6354.1791	1.046(29)	1.058	-1.1
2	6357.8139	2.086(17)	2.102	-0.8
3	6361.3435	3.068(34)	3.076	-0.3
4	6364.7676	3.922(44)	3.926	-0.1
5	6368.0861	4.620(26)	4.611	0.2
6	6371.2989	5.104(46)	5.103	0.0
7	6374.4058	5.400(58)	5.390	0.2
8	6377.4066	5.467(57)	5.443	-0.1
9	6380.3013	5.385(63)	5.370	0.3
10	6383.0896	5.121(77)	5.108	0.3
11	6385.7715	4.723(57)	4.721	0.0
12	6388.3467	4.252(55)	4.247	0.1
13	6390.8152	3.731(48)	3.725	0.2
14	6393.1767	3.183(44)	3.187	-0.1
15	6395.4312	2.673(56)	2.663	0.4
16	6397.5785	2.190(42)	2.175	0.7
17	6399.6184	1.751(45)	1.736	0.9
18	6401.5508	1.367(36)	1.356	0.8
19	6403.3756	1.037(28)	1.036	0.1
20	6405.0925	0.781(19)	0.775	0.8
21	6406.7016	0.566(15)	0.568	-0.4
22	6408.2025	0.404(31)	0.408	-1.0
23	6409.5952	0.282(17)	0.286	-1.4

[a]Observed intensities are averages of five Kitt Peak spectra converted to 296 K.
[b]Calculated via Eq. [4] using our intensity parameters from Table 1.
[c]Intensities in units of (cm^{-1}/cm-atm). $Q_{vr}(296)=107.428$.
[d](Sobs/Scalc-1)x100 percent Standard deviation equals 0.36 percent.
[e]Not included in fits.

Table 3. Intensity Parameters for the v=3←v=0 Band of $^{12}C^{16}O$.

Reference	$\|R\|^2$ x10^7(D^2)	C x10^2	D x10^5
Toth *et al.* [5]	1.84(10)	1.18(7)	18(10)
Bouanich *et al.* [6]	1.75(6)	1.18(7)[b]	18(10)[b]
Henningsen *et al.*[11]	1.697(17) [c]	1.323	
Picqué *et al.* [8,d]	1.6727(14)	1.204(5)	10.8(5)
Jacquemart *et al.* [12,d]	1.6730(12)	1.1996(39)	12.498(36)
This work	1.7127(25)	1.168(11)	10.65(79)
Calculated [e]		1.234	10.30

[a]Uncertainties for the last digits indicated represent one standard deviation.
[b]Adopted from Ref. (5).
[c]Corrected for isotopic abundance and Q_{vr} value used.
[d]References (8) and (12) used the same spectra.
[e]Taken from Ref. (18); to use these Herman-Wallis parameters include a cubic term, E = 4.98 x10^{-7} m^3, for |m| values up to 41.

Table 4. Self-broadening and self-shift coefficients.

m	γ^a	β^b	$-\delta^c$	m	γ^a	β^b	$-\delta^c$
				23	481(30)	224	
				22	506(63)	276	
				21	526(15)	222	740(49)
				20	519(5)	284	781(34)
				19	548(19)	320	616(118)
-18	575(27)	316	762(20)	18	570(25)	302	688(37)
-17	559(32)	273	723(66)	17	568(4)	342	668(33)
-16	578(18)	275	608(51)	16	576(9)	320	652(68)
-15	599(7)	272	686(86)	15	594(9)	320	654(23)
-14	607(11)	304	672(43)	14	601(4)	340	635(4)
-13	617(6)	348	677(47)	13	612(4)	342	605(36)
-12	617(7)	370	660(19)	12	618(3)	327	629(21)
-11	634(5)	334	664(18)	11	627(3)	370	599(8)
-10	649(5)	428	640(14)	10	636(3)	391	587(21)
-9	650(6)	412	657(24)	9	651(1)	442	610(13)
-8	661(3)	474	643(38)	8	660(3)	425	583(63)
-7	677(3)	476	620(28)	7	670(7)	505	588(23)
-6	692(5)	532	569(19)	6	691(4)	529	529(8)
-5	715(2)	625	540(24)	5	714(6)	605	541(29)
-4	745(3)	613	574(28)	4	733(9)	638	495(22)
-3	778(5)	564	432(20)	3	762(10)	600	428(52)
-2	829(2)	645	406(40)	2	819(17)	568	458(59)
-1	885(26)	689	449(48)	1	842(24)	727	254(38)

[a]Broadening units are $(cm^{-1}/atm)x10^{-4}$. Figures in parenthesis, expressed in the last digits, represent one standard deviation.

[b]Narrowing units are$(cm^{-1}/atm)x10^{-4}$. Errors on the order of ten-percent.

[c]Shift units are$(cm^{-1}/atm)x10^{-5}$. Figures in parenthesis, expressed in the last digits, represent one standard deviation. All shifts are negative.

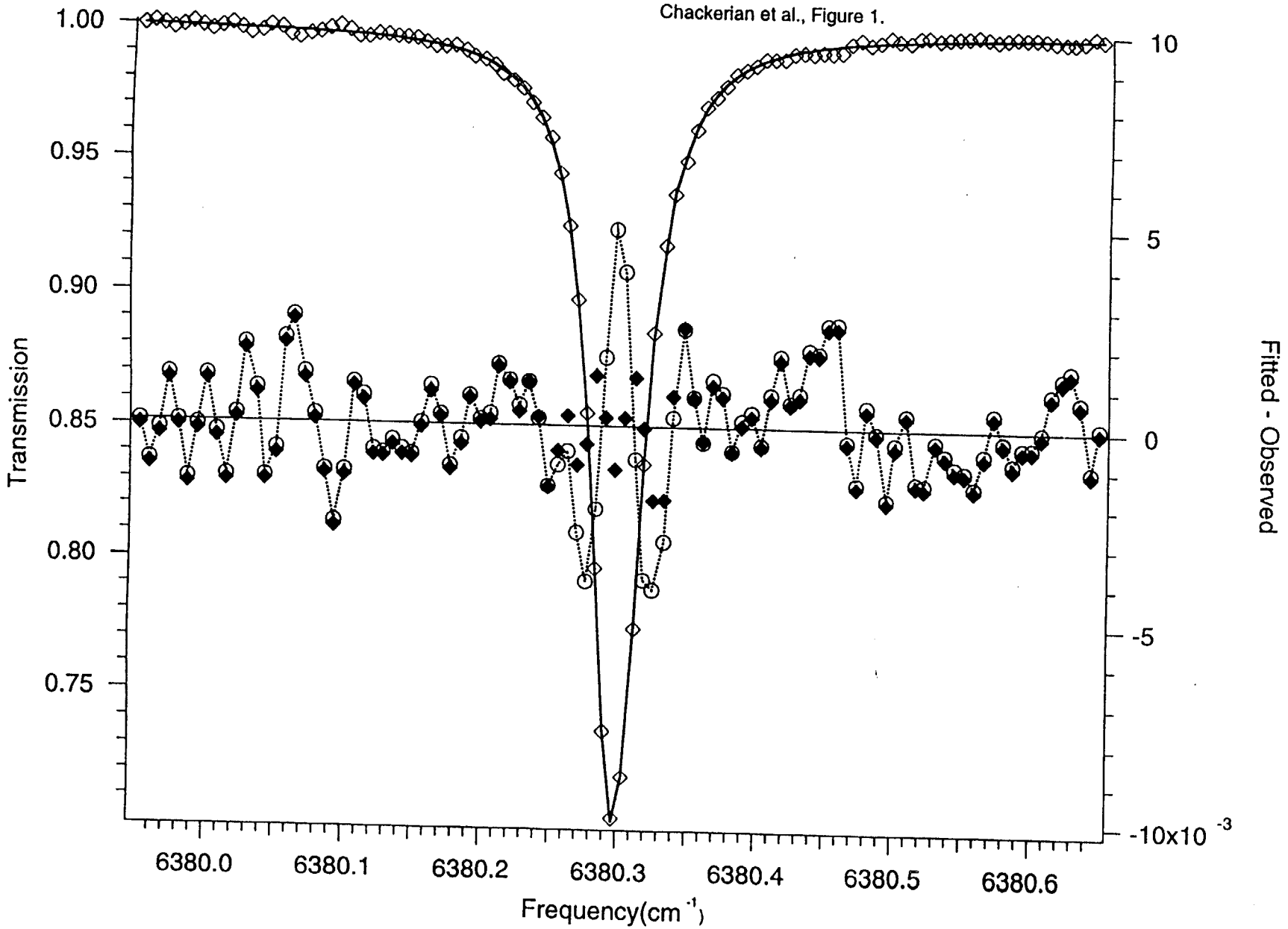
Chackerian et al., Figure 1.
1.00
0.95
0.90
0.85
0.80
0.75
Transmission
10
5
0
-5
-10x10 -3
Fitted - Observed
6380.0
6380.1
6380.2
6380.3
6380.4
6380.5
6380.6
Frequency(cm -1)

CHACKERIAN ET AL., FIGURE 2.

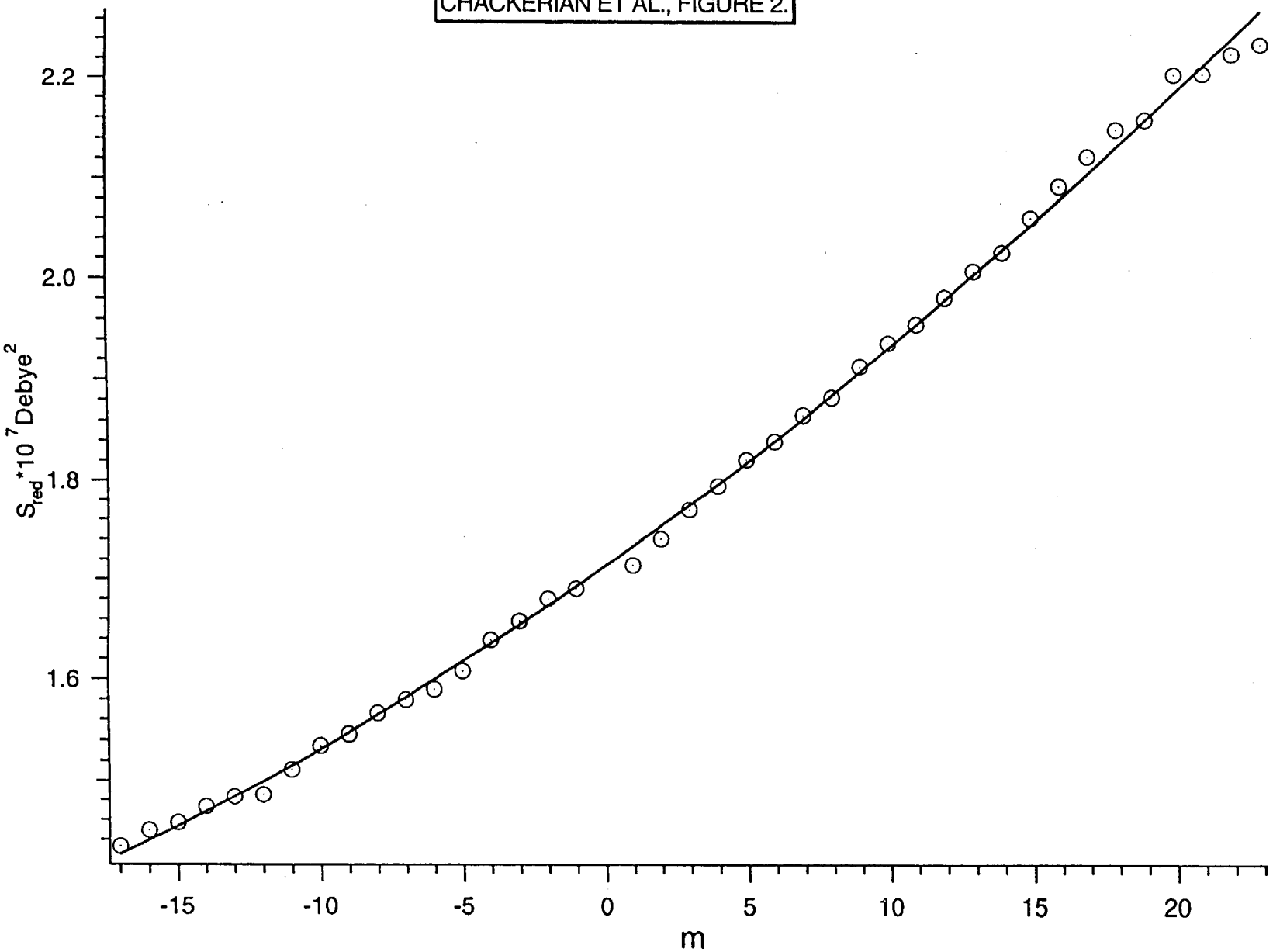

Chackerian et al.,Figure 3.

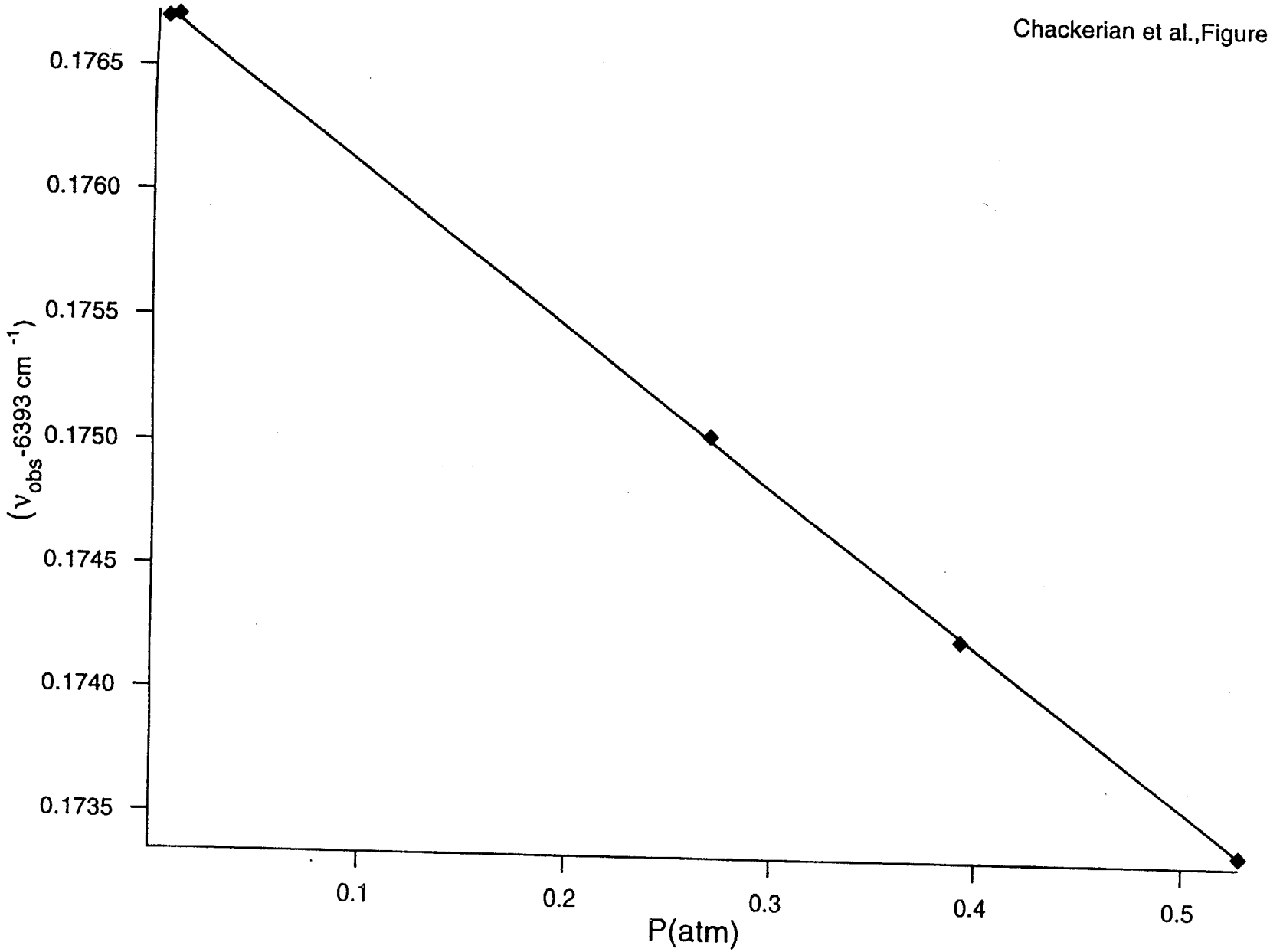

Chackerian et al.; Figure 4.

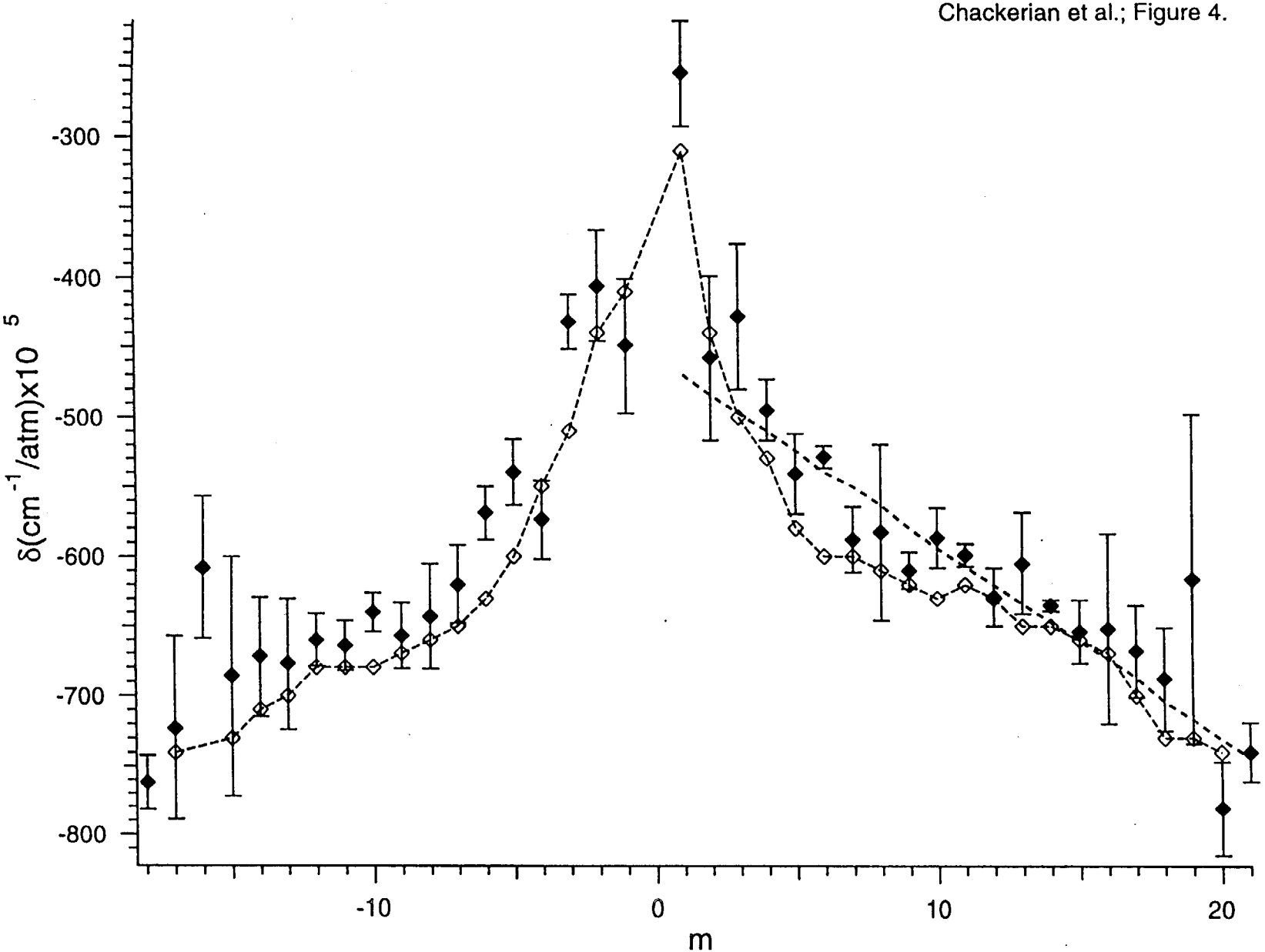

Chackerian et al., Figure 5.

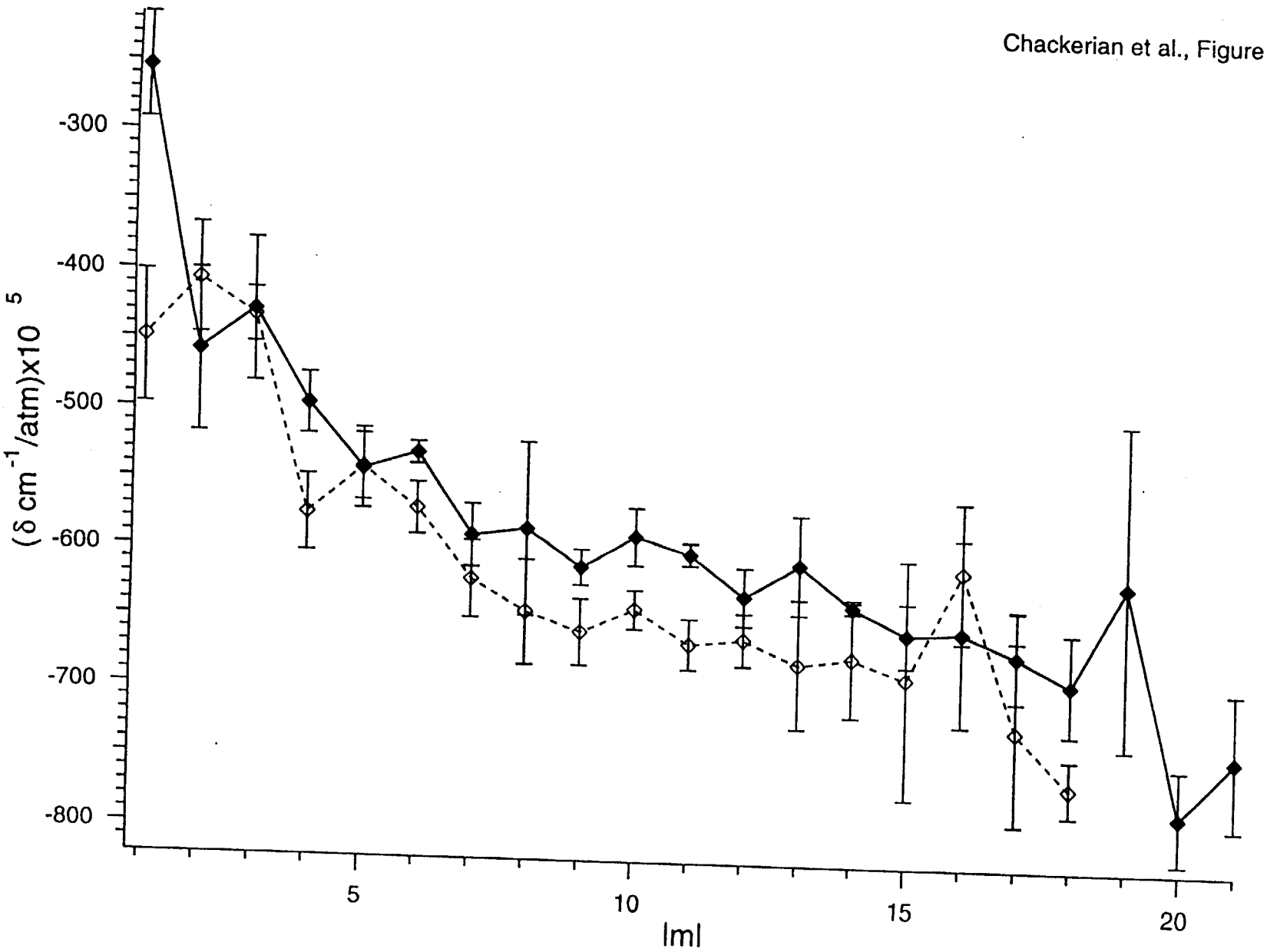

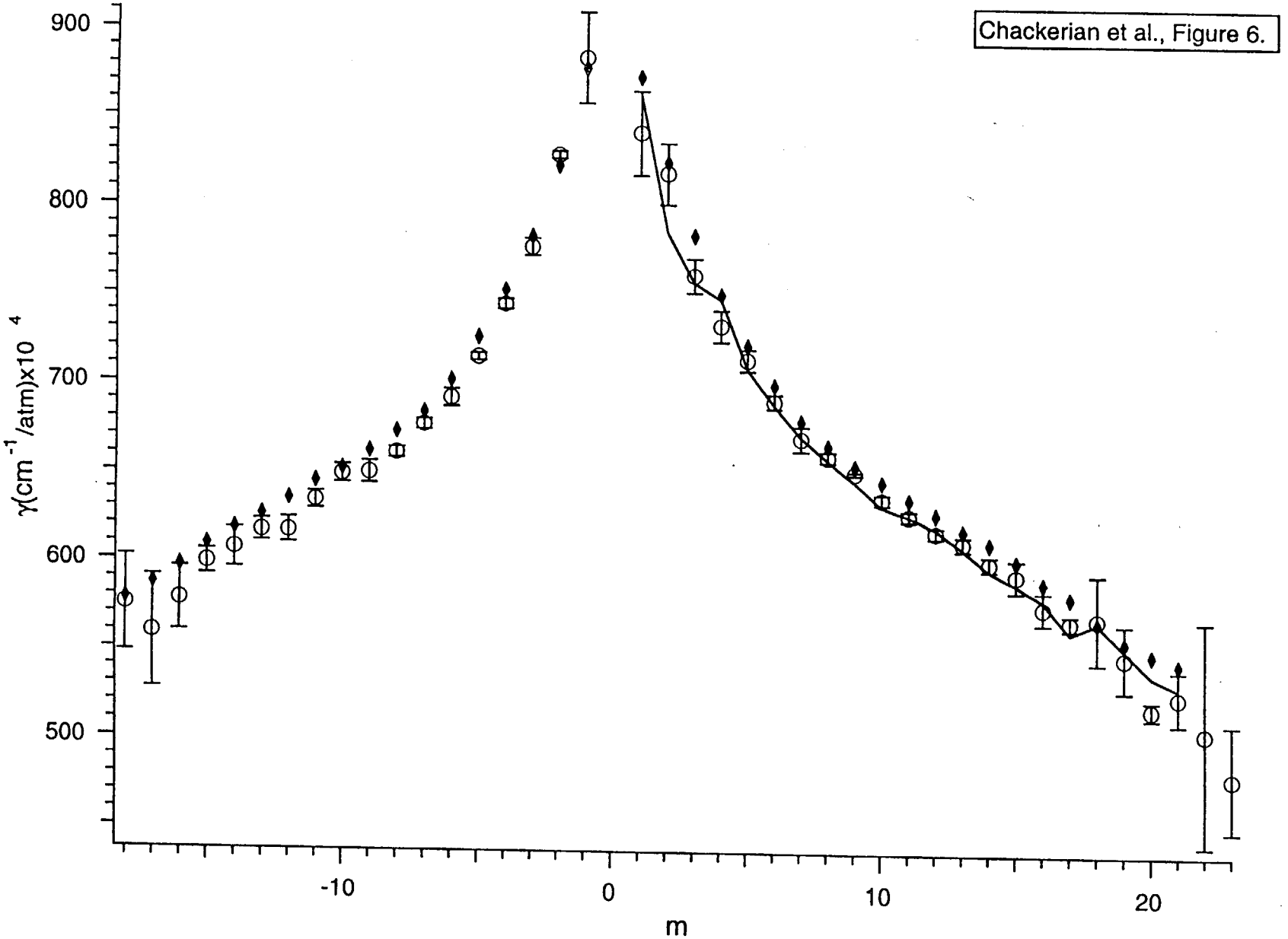
Chackerian et al., Figure 6.
900
800
700
600
500
γ(cm -1 /atm)x10 4
-10
0
10
20
m

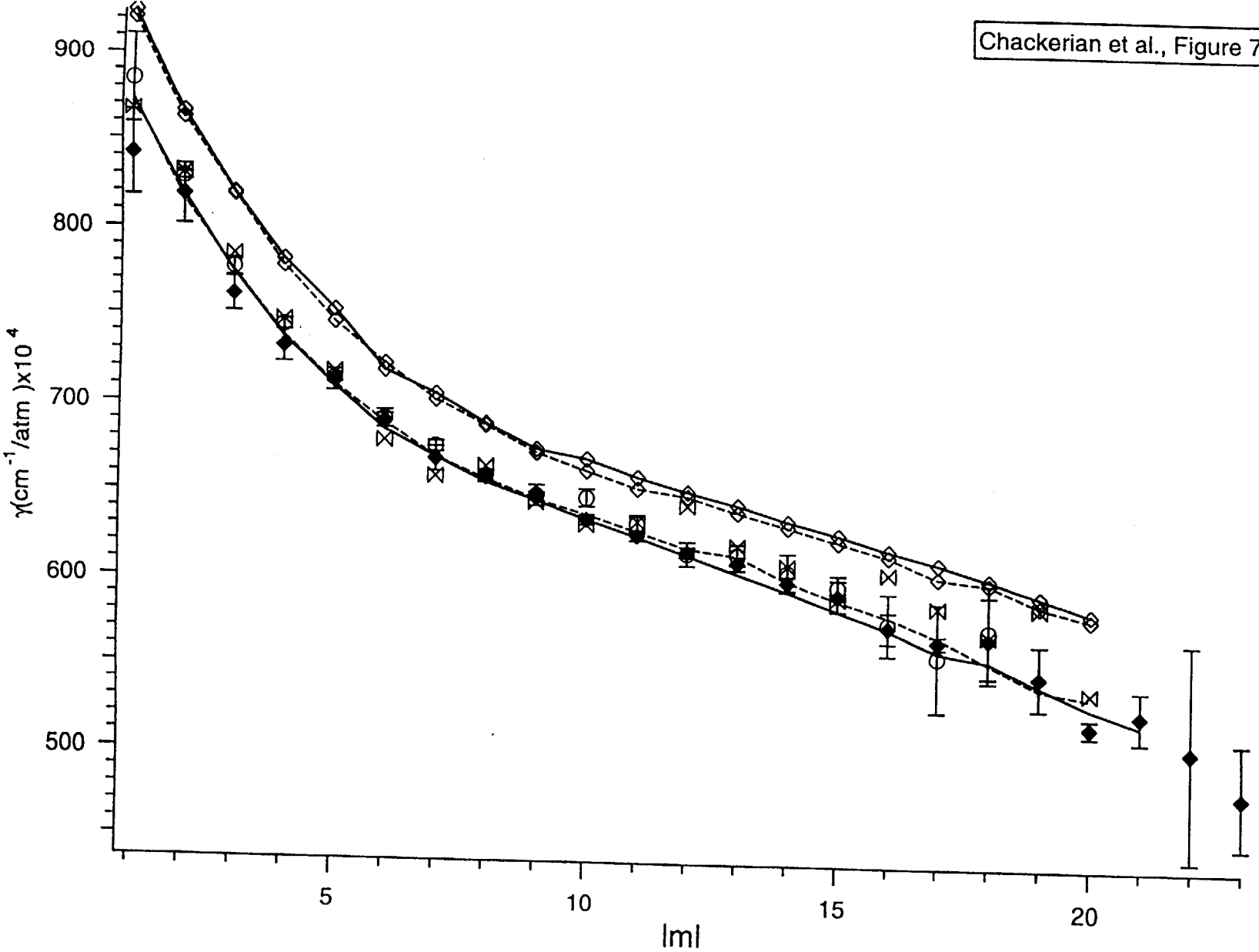
Chackerian et al., Figure 7.
900
800
700
600
500
γ(cm⁻¹/atm)x10⁴
5
10
15
20
|m|